A Microelectronic Sensor Device Powered by a Small Implantable Biofuel Cell †

Paolo Bollella,[a§] Inhee Lee,[b§] David Blaauw,[b]* Evgeny Katz[a]*

[a] *Department of Chemistry and Biomolecular Science, Clarkson University, Potsdam, NY 13699-5810, USA*

[b] *Department of Electrical Engineering and Computer Science, University of Michigan, Ann Arbor, MI 48109, USA*

[§] The authors equally contributed to the research project.

* Corresponding authors' contact information:

Evgeny Katz: ekatz@clarkson.edu, http://webspace.clarkson.edu/~ekatz/, +1-315-268-4421

David Blaauw: blaauw@umich.edu, https://blaauw.engin.umich.edu/, + 1-734-763-4526

† Supporting information for this article (additional data, photos of the experimental setup and comparison of power production by various implanted biofuel cells) is available on the WWW under https://....

Biocatalytic buckypaper electrodes modified with pyrroloquinoline quinone (PQQ)-dependent glucose dehydrogenase and bilirubin oxidase for glucose oxidation and oxygen reduction, respectively, were prepared for their use in a biofuel cell. A small (millimeter-scale; $2 \times 3 \times 2$ mm^3) enzyme-based biofuel cell was tested in a model glucose-containing aqueous solution, in human serum, and as an implanted device in a living gray garden slug (*Deroceras reticulatum*), producing electrical power in the range of 2-10 μW (depending on the glucose source). A microelectronic temperature-sensing device equipped with a rechargeable supercapacitor, internal data memory and wireless data downloading capability was specifically designed for activation by the biofuel cell. The power management circuit in the device allowed the optimized use of the power provided by the biofuel cell dependent on the sensor operation activity. The whole system (power-producing biofuel cell and power-consuming sensor) operated autonomously by extracting electrical energy from the available environmental source, as exemplified by extracting power from the glucose-containing hemolymph (blood substituting biofluid) in the slug to power the complete temperature sensor system and read out data wirelessly. Other sensor systems operating autonomously in remote locations based on the concept illustrated here are envisaged for monitoring different environmental conditions or can

be specially designed for homeland security applications, particularly in detecting bioterrorism threats.

1. Introduction

Enzyme-based biofuel cells[1] extracting electrical power from abundant biomolecules have been studied for several decades[2] to resolve fundamental bioelectrochemical problems for efficient electron exchange between enzyme active centers and electrode conducting supports.[3] Engineering problems in constructing biofuel cells are mostly related to increasing the power density generated by electrochemical devices and extending their operational time.[4,5] While some scientific/engineering papers use "green energy," "sustainable power sources," "cheap electrical power" and other politically motivated wording as justification for biofuel cell research,[6] it should be clearly understood that biofuel cells, particularly those based on enzyme biocatalysis, will likely never produce sufficient power to contribute any meaningful amount of power to the national power grid. Also, the electrical power produced through biological reactions is unlikely to be cheap, particularly when using expensive enzymes with limited operational time. Therefore, the real motivation for the research in biofuel cells is their promise for powering implantable biomedical devices[7] or sensors/biosensors,[8] particularly in remote locations where locally produced electrical power extracted from environmentally available biological sources[9] can be beneficial. Since the amount of power produced is rather small,[10-12] the cost of this power is not critically important, while other parameters, like operation in a biological environment, are becoming more important. With a clear understanding of this motivation, the research focus has moved to implantable biofuel cells surgically introduced in biological tissue of living animals[13-16] (used as models for future use in humans) and wearable biofuel cells[17,18] located externally on a body, being easily replaced when the operational resource is exhausted. Differently constructed enzyme-based biofuel cells have been tested *in vitro* in human serum solution [19,20] or whole blood[21-23] and *in vivo* in various living species, such as insects,[24] snails,[25] clams,[26] lobsters,[27] rats,[28,29] rabbits,[30,31] etc. Wearable biofuel cells have been reported that are placed on human skin and powered by sweat[32,33] or in an eye and powered by tears.[34,35]

The next highly important research direction is interfacing implantable or wearable biofuel cells with various electronic devices that consume power generated by the biofuel cells.[36-40] While most of the studied bioelectronic systems have included only model devices, such as an electronic watch,[27] digital thermometer,[41] and light-emitting diode (LED),[41] some of the

electronic devices powered by implantable biofuel cells, e.g., a pacemaker,[20] glucometer,[42] and smart contact lenses,[34,43] are close to the expected future biomedical applications. In designing integrated bioelectronic systems composed of a biofuel cell producing electrical power and an electronic device consuming this power, the major problem is the insufficiency of the power produced. When the connected electronic device needs continuously provided power, the problem can be solved by improving the efficiency of the connected biofuel cell (not easy) or by increasing the biofuel cell size (easy but not practical for implantable systems). The required power is often limited by the threshold needed for the operation of the DC-DC converter ("charge pump"), which increases the voltage generated by a biofuel cell to the level required by the power-consuming device. In most of the systems studied,[15] the power required for continuous (without interruption) operation of any practically important electronic device was produced by relatively large (several cm^2) biocatalytic electrodes, which are too big for implantable bioelectronic systems.[20] Another much more practical solution has been suggested for systems that are activated periodically or "duty cycled". This approach uses the standby time intervals for accumulating electrical energy in a rechargeable battery or supercapacitor.[44-46] The technical question remaining is how small can a biofuel cell be that provides sufficient power for activation of a microelectronic device that operates periodically. The answer depends mostly on the efficiency of the microelectronic device. The present paper offers an experimental answer to this question using a highly efficient microelectronic device, which includes a power management system equipped with a supercapacitor.

Rapid progress in microelectronics has resulted in small but very powerful computing and sensing systems. Nowadays, people are using centimeter-scale devices in their daily lives (e.g., smartphones), and millimeter/micrometer-scale systems are on the horizon.[47,48] In such miniature systems, battery size and thus battery capacity are highly limited, and the available energy stored in a battery is a significant limitation.[47,48] We developed a millimeter-scale custom designed system with low-power circuits that consumes current in the μA range in the active mode for time intervals of ca. 100 ms and current in the nA range while in standby mode for tens of seconds. Relying on a millimeter-size thin-film battery, the proposed system can operate for about a month.[49] To extend this system lifetime, replacing a battery is difficult since the system needs to be fully encapsulated for physical protection and, in any case, replacing batteries *in vivo*

is impractical. Thus, these millimeter-scale systems must include an energy-harvesting feature and a rechargeable battery.[50] In this way, the microelectronic devices can become energy autonomous by recharging the battery using energy harvested from sources available in the operational environment. However, the system lifetime is still limited by the rechargeable battery degradation, as its capacity decrease and internal resistance increase with each cycle of charging/discharging.[51] A supercapacitor is a good alternative to a battery since its performance degradation is negligible even after a large number of charging/discharging cycles compared with that of a miniature rechargeable battery. In this paper, we demonstrate a temperature-logging millimeter-scale system that is based on a supercapacitor and is recharged with a millimeter-size biofuel cell. A supercapacitor typically suffers from limited energy density, but that challenge is overcome by an efficient biofuel cell and low-power circuits in this system. This integrated bioelectronic system composed of a power-producing biofuel cell and a power-consuming sensor device, both millimeter-scale, was studied and reported in this paper. While many other implanted biofuel cells have been reported, the present work aims at demonstration of the implanted biofuel cell operation together with a microelectronic device. The size of the implanted biofuel cell matches the size of the microelectronic device and the use of a slug as a host organism is based on its availability in the natural environment in the season when the experimental work was done. Notably, the slug is only an example for the integrated biofuel cell – microelectronic device. It should be noted that the enzymes used in the present study, PQQ-dependent glucose dehydrogenase (PQQ-GDH) in the anode and bilirubin oxidase (BOx) in the cathode, are not the only possible enzymes for the use in the studied implantable biofuel cell. Some other enzymes, particularly those operating without redox mediators (through direct electron transfer), might be successfully used, but their application was outside the scope of the present study.

2. Experimental

2.1. Materials

PQQ-dependent glucose dehydrogenase (PQQ-GDH; E.C. 1.1.5.2) from a microorganism not specified by the company was purchased from Toyobo Co., Japan. Bilirubin oxidase (BOx; E.C. 1.3.3.5) from *Myrothecium verrucaria* was kindly donated by Amano Enzyme Inc., U.S.A. 3-Thiopheneacetic acid, 3-methoxythiophene, β-D-glucose, 4-(2-hydroxyethyl)piperazine-1-

ethanesulfonic acid (HEPES buffer), 2-(*N*-morpholino)ethanesulfonic acid (MES buffer), *tris*(hydroxymethyl)aminomethane (TRIS buffer), *N*-(3-dimethylaminopropyl)-*N′*-ethylcarbodiimide hydrochloride (EDC), *N*-hydroxysuccinimide (NHS), sterile-filtered human serum from human male AB plasma USA origin, and other standard organic and inorganic chemicals and reactants were purchased from Millipore Sigma (formerly Sigma-Aldrich) and used as supplied. Ultrapure water (18.2±0.2 MΩ·cm) from a NANOpure Diamond (Barnstead) source was used in all of the experiments. The live specimens of the gray garden slug (*Deroceras reticulatum*)[52] used in this study were collected in the Clarkson University park (NY, USA). The specimens measured on average 3 cm in length when extended (1.5−2 cm when retracted), which is usual for adults of this species. The slugs were held in a box containing dirt with fruit and grass.

2.2. Electrode preparation

Buckypaper composed of compressed multiwalled carbon nanotubes (MWCNTs; Buckeye Composites, NanoTechLabs, Yadkinville, NC) was used as the electrode material (2 mm × 3 mm; geometric area = 0.06 cm^2). Indium-tin oxide (ITO; 20±5 Ω/sq surface resistivity; Millipore Sigma) was used as the conducting support for the mechanical reinforcement of the buckypaper, which was attached to ITO using silver conductive epoxy glue (MG Chemicals, Surrey, Canada). First, the electrodes were modified with a thiophene-based polymer. Electropolymerization of thiophene monomers was performed by using a potentiostatic pulse method, adopting the following parameters: 1.4 V oxidation potential and 0.8 s oxidation pulse time, –0.3 V reduction potential, 0.1 s reduction pulse time, and 677 pulses, which means a total experiment time of 600 s. The solution used for the electropolymerization included two thiophene-derivative monomers, 3-thiopheneacetic acid (67 mM) and 3-methoxythiophene (33 mM), and supporting electrolyte KCl (100 mM) in aqueous solution containing 5% (v/v) acetonitrile. The electropolymerization procedure was optimized based on the results reported in the literature.[53,54] After the polythiophene electrodeposition, the modified electrode was repeatedly rinsed with water, and four cyclic voltammogram scans (100 mV/s, between −0.2 V and 0.5 V) in 5 mM MES buffer, pH 6.5, were performed to remove the monomer residues and acetonitrile from the polymer layer. Afterwards, the modified electrodes were incubated with a mixture of 25 mM NHS and

100 mM EDC (to activate -COOH groups of the polymer) under moderate shaking for 1 h at room temperature (23 ± 2 °C) and subsequently rinsed with phosphate buffer (50 mM, pH 7.4, containing 100 mM Na_2SO_4). PQQ-GDH and BOx were used to modify the anode and cathode, respectively. The polymer-modified electrodes with the activated carboxylic groups were immediately incubated with enzyme solutions, 2.4 $mg \cdot mL^{-1}$ for PQQ-GDH (in 10 mM HEPES buffer, pH 6.0, containing 6 mM $CaCl_2$) and 3.7 $mg \cdot mL^{-1}$ for BOx (10 mM TRIS buffer, pH 7, containing 100 mM Na_2SO_4), for 1 h at room temperature under moderate shaking. The modified electrodes were stored (4 ºC) in phosphate buffer (50 mM, pH 7.4, containing 100 mM Na_2SO_4) until used in the biofuel cell.

2.3. Electrochemical characterization of the modified electrodes

Cyclic voltammetry measurements were carried out with an ECO Chemie Autolab PASTAT 10 electrochemical analyzer using the General Purpose Electrochemical System (GPES 4.9) software package. The working electrode was made of buckypaper attached to an ITO support (0.06 cm^2 geometrical area) modified with a polythiophene layer functionalized with PQQ-GDH or BOx. A BASi Ag|AgCl|3M KCl electrode served as the reference electrode, and a graphite slab was used as the counter electrode. Cyclic voltammograms were recorded at a potential scan rate of 1 $mV \cdot s^{-1}$ in an electrolyte solution composed of 50 mM phosphate buffer, pH 7.4, containing 100 mM Na_2SO_4. Cyclic voltammograms of the PQQ-GDH-electrode were obtained in the absence and presence of 5 or 20 mM glucose while cyclic voltammograms of the bilirubin oxidase-electrode were obtained in the absence and presence of oxygen (in equilibrium with air). Anaerobic conditions were achieved by purging the solution with argon. Note that the PQQ-GDH-modified electrode operated in the presence of air since the PQQ-GDH enzyme is O_2 insensitive.

2.4. Biofuel cell measurements

In the preliminary experiments, polarization curves of the biofuel cell were recorded at different glucose concentrations (5 mM, 10 mM and 20 mM) in phosphate buffer (50 mM, pH 7.4, containing 100 mM Na_2SO_4 and oxygen under equilibrium with air). Then, the biofuel cell was also tested in a human serum solution. Finally, the implantable electrodes were inserted into the slugs through two holes cut with a small knife in a dorso-posterior part of the body and placed

into the hemolymph between the body wall and heart, dorsal to the visceral mass with a distance between the electrodes of ca. 2 mm (varied in different specimens by ±1 mm). The geometrical area of the electrodes immersed in the hemolymph was 0.06 cm^2. The volume of the biofuel cell was ca. 0.012 cm^3. The volume was calculated as the inner volume (operational volume inside the cell) based on the distance between the biocatalytic electrodes (the anode and cathode). The voltage and current generated by the biofuel cell were measured with a multimeter (Meterman 37XR) with a variable resistance used as an external load. All measurements were performed at ambient temperature (23 ± 2 ºC).

2.5. Microelectronic device operating as a temperature sensor

The batteryless temperature sensor measures ambient temperature and saves the data in internal memory (8kByte SRAM), and a user can wirelessly download the results later using optical or radio frequency (RF) communication. All operations can be powered by energy from the biofuel cell with the help of a supercapacitor operating as an energy buffer.

As shown in Figure 1, the microelectronic device consists of stacked chips (1.4 × 2.8 × 1.0 mm^3) and a supercapacitor (3.2 × 2.5 × 0.9 mm^3) packaged in a ceramic pin grid array (PGA) for ease of testing. The stack of chips includes 8 integrated circuit chips, including a 'charge pump,' 'power management,' 'memory,' 'decoupling capacitors,' 'processor,' 'radio,' 'temperature sensor & timer,' and 'optical receiver.' They are all fabricated in 180-nm CMOS technology and were custom designed to construct a millimeter-scale sensor system. The circuits on the chips are designed with the highest priority placed on low power consumption and operate with less power on average than what the biofuel cell can provide.

Figure 2 shows an electronic diagram of the designed biofuel cell-powered miniature system. The biofuel cell extracts electrical power from glucose/O_2-containing model solutions (phosphate buffer or human serum) or from hemolymph in a living slug with implanted biocatalytic electrodes. A 'charge pump' chip harvests energy from the biofuel cell, which produces a low voltage (e.g., 0.4 V) (Vbfc) and converts it to a higher voltage (e.g., 2.4 V) (Vcap) to recharge the supercapacitor. The charge pump has a reconfigurable voltage conversion ratio, enabling the biofuel cell to operate at its maximum power point.[50] Depending on the biofuel cell output

power, the switching frequency of the charge pump automatically changes to maintain high efficiency in energy harvesting. Vbfc and thus Vcap vary depending on glucose concentration. Under such a varying Vcap, the circuits of other chips cannot operate properly. Hence, the 'Power Management' chip takes this varying Vcap and generates a set of three regulated voltages: 0.6 V, 1.2 V, and 3.6 V.[55] The power management chip includes 3 up/down charge pumps, and their switching frequencies adapt to the amount of current draw from the load circuits. For example, the power management charge pumps change their configuration to significantly faster in active mode than in standby mode. A 'Decoupling Capacitor' chip provides decoupling capacitance in the nF range to further stabilize the three output voltages (0.6 V, 1.2 V, and 3.6 V) and to suppress high frequency noise due to the instantaneous current draw from the circuits in the supplied chips. The 'Processor' chip manages the temperature logging operation using an ARM Cortex-M0 processor and 8 kByte memory.[47] The 'Memory' chip stores the measured temperature data up to 8k samples using 16 kByte memory. The 'Temperature Sensor & Timer' chip converts the temperature to a digital code with 0.05 ^{o}C temperature inaccuracy from 0 ^{o}C to 105 ^{o}C using both a temperature-sensitive and temperature-insensitive clock generator.[56] Finally, the timer on this chip accurately sets the period between two adjacent temperature measurements within 1% accuracy across temperatures.[57] This sensor communicates with a user by optical and radio methods. For programming, a user sends an optical signal to a photovoltaic cell on the 'Optical Receiver' chip, and the signal is converted to a digital format in the 'Processor' chip.[47] On the other hand, the 'Radio' chip transmits a 900 MHz radio signal to send out the measured data. The 'Radio' chip transmits data by near-field inductive coupling using a current limiter, a decoupling capacitor, a controller, a pulse generator, a power oscillator and an on-chip antenna.[58] The current limiter and decoupling capacitor help to limit the current draw from the 'Power Management' chip at the maximum power condition. The controller and pulse generator trigger the power oscillator and on-chip antenna to send a radio signal using pulse position modulation. An on-chip inductor supports radio communication up to 10 cm. A base station wirelessly receives the transmitted radio signals and saves them in a digital format. Storing measured data in memory and transmitting it later enables the sensor to operate apart from the base station while measuring temperature. This is an advantage for an implantable device, a target application of this prototype sensor.

In the microelectronic temperature-sensing device, the leakage current of the supercapacitor (hundreds of nA) dominates the average power consumption. Except for the leakage current, the power consumption is mainly determined by the sleep mode. In the sleep mode, the 'Charge Pump', 'Decoupling Capacitor', 'Processor', 'Memory' and 'Radio' chips consume 11.2 nW, 0.36 nW, 6.8 nW, 1.3 nW and 0.37 nW, respectively. The 'Power Management' chip has the power conversion efficiency of 60%.[50] Thus, the microelectronic device, except for the supercapacitor, consumes 34.0 nW.

Figure 3 shows the setup used to test the different components individually and also, when configured as a complete system, autonomous system operating without external power. The shown setup includes the biofuel cell operating with an aqueous model solution (phosphate buffer) containing glucose and O_2. A sourcemeter (Keithely 2401 Sourcemeter) is used to characterize the sensor by measuring current consumption at a given voltage and can also accelerate tests by pre-charging the supercapacitor. Another sourcemeter is used to characterize the energy harvesting of the sensor by mimicking a biofuel cell. An electrometer (Keithely 6514 System Electrometer) is used to monitor 1.2 V from the 'Power Management' chip to confirm that the sensor works properly by providing voltage to the load circuits. To avoid impacting the low-power circuits, a high impedance electrometer is used. To monitor the voltage of the supercapacitor (Vcap), the node is connected to an analog buffer (Texas Instruments, OPA4354AIDR) powered by a power supply (Agilent E3630A) to avoid influence on this low-power circuit. Then, the voltage is converted to a digital format by an analog-to-digital converter module (National Instruments, NI-9229 & NI cDAQ-9171). The results are displayed on the monitor using a LABVIEW program. A laptop and a custom light programing module are used to generate an optical signal and program the sensor. A universal software radio peripheral (USRP) (Ettus, USRP X310), a custom antenna and the same laptop are used to wirelessly download the measured data from the sensor.

3. Results and Discussion

Both enzymes, PQQ-dependent glucose dehydrogenase (PQQ-GDH)[25,59] and bilirubin oxidase (BOx)[60,61] used for catalyzing the anodic and cathodic reactions in the biofuel cell, respectively,

are known for direct (non-mediated) electron communication with electrodes, especially when using buckypaper as the conducting support.[62-65] While PQQ-GDH and BOx can operate as electrocatalysts at modified electrodes without electron transfer mediators, the use of a polythiophene sub-layer can further promote electron transfer and enhance the anodic and cathodic currents catalyzed by PQQ-GDH and BOx.[53,54] Figure 4 shows schematically the electropolymerization process for preparation of the polythiophene layer, further functionalized with the enzymes PQQ-GDH and BOx for preparing the anode and cathode, respectively. The enzymes were attached covalently to the carboxylic groups in the polymer film (note the use of 3-thiopheneacetic acid as a co-precursor in the polymerization process; see description of the control experiment performed without EDC in the Supporting Information). The enzyme-modified buckypaper electrodes, mechanically reinforced by attaching to ITO supports, were studied by cyclic voltammetry for electrocatalytic glucose oxidation and O_2 reduction, Figure 5. The PQQ-GDH-modified electrode demonstrated electrocatalytic glucose oxidation at potentials more positive than –90 mV, Figure 5A, and the BOx-modified electrode electrocatalytically reduced O_2 at potentials more negative than +510 mV, Figure 5B. The values –90 mV and +510 mV for both electrodes were measured as open circuit potentials (OCP). Based on the cyclic voltammetry measurements and the OCP numbers, the open circuit voltage (OCV) in the biofuel cell composed of the PQQ-GDH and BOx electrodes can be expected to be ca. 600 mV, Figure 5.

With the goal of power production by a small (millimeter-scale) implantable biofuel cell, we assembled a biofuel cell with 2 mm × 3 mm (0.06 cm^2 geometrical area) enzyme-modified electrodes. Prior to implantation of the electrodes into living species, the biofuel cell performance was studied with a 20 mM glucose/O_2 aqueous solution (50 mM phosphate buffer, pH 7.4, containing 100 mM Na_2SO_4), Figure 6A-C. The biofuel cell demonstrated an OCV of 600 ± 10 mV (as expected), a short circuit current of 48 ± 2 μA (ca. 800 μA/cm^2 short circuit current density vs. geometric area) and a maximum power release of 10.5 ± 0.5 μW at 25 kΩ load resistance and 0.39 V. Taking into account the electrode area of 0.06 cm^2 and the distance between the biocatalytic electrodes of ca. 0.2 cm, the volume of the biofuel cell was ca. 0.012 cm^3, thus resulting in a maximum power density of 875 ± 5 μW/cm^3. The power output was

dependent on the glucose concentration, Figure 7, decreasing as the glucose concentration decreased, as expected.

In the next preliminary experiment, the biofuel cell was tested with a human serum solution containing approximately 6 mM glucose.[20,66] The output voltage, current and power were smaller than those obtained with the buffer solution, Figure 6D-F, due to lower glucose concentration and much higher viscosity of the biofluid. Still the maximum power release was rather impressive, 660 ± 20 μW/cm^3, smaller only by factor of 1.3 compared to that obtained in the aqueous glucose solution. The biofuel cell operation with the human serum solution provides important information for future biomedical applications; however, *in vivo* testing is also desirable. Since the implantation of the biofuel cell into a human body is not possible at the present stage, particularly in a chemical lab, we performed our experiments using slugs (invertebrate terrestrial mollusks).[52]

The biocatalytic electrodes were inserted in the living slug tissue, and the implanted biofuel cell operated with hemolymph (biofluid equivalent to blood in invertebrates) containing glucose and O_2, Figure 8. The glucose concentration in the hemolymph has seasonal variation, with a typical concentration of ca. 0.7 mM in summer,[67] when the experiments were performed. While the voltage, current and power release were further decreased, the maximum power was measured as 2.4 ± 0.1 μW (ca. 200 μW/cm^3), only smaller by a factor of ca. 2.4 compared with the power produced in a buffer solution containing 5 mM glucose (Figure 7), which is expected due to the lower glucose concentration in the hemolymph. An important question is if the power produced by the small implanted biofuel cell is sufficient for activation of the microelectronic device. The answer will depend on the power demanded by the device. It should be noted that the slug was alive during the experiments and survived after them.

After the biofuel cell and microelectronic sensor were characterized in terms of current, voltage and power, the biofuel cell was connected to the microelectronic sensor and the sensor operated autonomously powered only from the biofuel cell. Figure 9A shows the measured voltage of the supercapacitor (Vcap in Figure 2) over time. In the beginning, the sensor starts to measure temperature every 11 seconds. However, since the biofuel cell is not yet activated and the sensor

consumes energy from the supercapacitor, its voltage decreases gradually. During the higher current draw, when the sensor is in the active mode, there is a short downward spike in the voltage due to the internal resistance of the supercapacitor. When the biofuel cell is activated, as noted in the figure, the sensor 'charge pump' chip activates and start to recharge the supercapacitor using energy from the biofuel cell. At this point the voltage starts to increase again since the harvested power is larger than the average power consumed by the sensor. The rising voltage indicates that the system is energy autonomous and can continue the operation using the power provided by the implanted biofuel cell. The supercapacitor supports the different active operations of the sensor, including programming of the sensor (at the very start of the curve) and wireless data downloading (at the end of the curve) without significant voltage decrease (< 18 mV drop due to internal resistance), ensuring correct system operation. Figure 9B shows the temperature measurements recorded by the sensor, logged in its internal memory and readout wirelessly and saved in the laptop. The sensing device can operate autonomously as long as the biofuel cell is active and the energy source (glucose in the hemolymph) is available. The present biofuel cell was not studied for long-term operation, however, it demonstrated reproducible power production over several days. It should be noted that similar kinds of biofuel cells have been reported to successfully operate for over 1 year,[68] which is much longer than can be obtained with a battery of a comparable size. The microelectronic device, despite the fact that it is a very sophisticated system, can be produced in many copies with reproducible features. The manufacturing process is rather standard for the state-of-the-art in microelectronics.

4. Conclusions

Enzyme-based biofuel cells implanted in different living species (ranging from invertebrates[24-27] to mammals[28-31]) have been reported recently. The power produced by them was in the μW range depending on the bioelectrode size and the "biofuel" (e.g., glucose) concentration in the biofluid (see Table 1 in the Supporting Information). It should be noted that the power density (power normalized to the electrode surface, $\mu W/cm^2$, or to the biofuel cell volume, $\mu W/cm^3$) is not the parameter that is important for practical use of the biofuel cell. Indeed, even if the power density is high but the biofuel cell is very small, the total power produced might be insufficient for activating any connected electrical/electronic device. Therefore, the total power produced,

particularly for small biofuel cells, is the critical parameter that should meet the power requirements of the connected electrical load.

Very small enzyme-based biofuel cells (micrometer-scale) have been reported previously;[69] however, there are not many examples of their operation with a connected electrical/electronic load consuming the produced power. Particularly, sophisticated "smart" microelectronic sensors with wireless data readout have never been powered by small biofuel cells. The present work combined two challenging research goals: designing a small size biofuel cell and assembling a "smart" microelectronic device with its harvesting ability and power consumption designed for the available power. The exemplified power source was a slug, but many other potential environmental sources of energy exist.[9] The process limiting power generation by an implanted biofuel cell, which could be at the biocathode or bioanade, depends on many parameters. Some of them can be controlled by preparing the electrodes (changing the activity/amount of the immobilized enzymes), but some are controlled by physiological processes in the living host species (i.e. slug in the present study).[25] It has been shown that feeding a snail (used in our previous study) increases the power production due to elevated glucose concentration produced physiologically. The physiological variation of glucose and oxygen concentrations may change the limiting process in the implanted biofuel cell.

Autonomously operating microelectronic devices continuously powered by small biofuel cells will be beneficial for various environment-monitoring functions, including biosensors designated specifically for homeland security and military applications. Further miniaturization of the sensor device and connected biofuel cell would allow their operation as implantable biomedical devices. The microelectronic device can accommodate the biocatalytic electrodes directly in the structure of the device, thus further reducing the device size and eliminating unnecessary wiring connecting the biofuel cell and the electronic device. For microelectronic production convenience, the biofuel cell can be prepared as an "abiotic" device[70] with the electrocatalytic electrodes modified with inorganic catalytic species (e.g., noble metal nanoparticles) instead of the enzymes used in the present study. "Abiotic" biofuel cells can extract electrical energy from biological sources, e.g., using glucose as the "fuel."[71] Overall, the present first report of a biofuel

cell combined with a microelectronic device has many different potential technological extensions for various applications.

Conflicts of interest

There are no conflicts to declare.

Keywords: biofuel cell; microelectronic device; sensor; implantable cell; power management

References

1 P. Atanassov, G. Johnson, H. Luckarift (Eds.), *Enzymatic fuel cells: From fundamentals to applications*, Wiley-VCH, Weinheim, Germany, **2014**.

2 M. Rasmussen, S. Abdellaoui, S. D.Minteer, *Biosens. Bioelectron.* **2016**, *76*, 91–102.

3 I. Willner, E. Katz, *Angew. Chem. Int. Ed.* **2000**, *39*, 1180–1218.

4 A. J. Gross, X. Chen, F. Giroud, C. Abreu, A. Le Goff, M. Holzinger, S. Cosnier, *ACS Catal.* **2017**, *7*, 4408–4416.

5 M. J. Moehlenbrock, S. D. Minteer, *Chem. Soc. Rev.* **2008**, *37*, 1188–1196.

6 S. Aquino Neto, A. R. De Andrade, *J. Braz. Chem. Soc.* **2013**, *24*, 1891–1912.

7 E. Katz (Ed.), *Implantable Bioelectronics - Devices, Materials and Applications*, Wiley-VCH, Weinheim, Germany, **2014**.

8 C. Gonzalez-Solino, M. Di Lorenzo, *Biosensors* **2018**, *8*, art. No. 11

9 K. MacVittie, T. Conlon, E. Katz, *Bioelectrochemistry* **2015**, *106*, 28–33.

10 V. Andoralov, M. Falk, D. B. Suyatin, M. Granmo, J. Sotres, R. Ludwig, V. O. Popov, J. Schouenborg, Z. Blum, S. Shleev, *Sci. Rep.* **2013**, *3*, art. No. 3270.

11 S. C. Barton, J. Gallaway, P. Atanassov, *Chemical Rev.* **2004**, *104*, 4867–4886.

12 A. Heller, *Phys. Chem. Chem. Phys.* **2004**, *6*, 2009–2016.

13 A. Zebda, J.-P. Alcaraz, P. Vadgama, S. Shleev, S. D. Minteer, F. Boucher, P. Cinquin, D. K. Martin, *Bioelectrochemistry* **2018**, *124*, 57–72.

14 S. Cosnier, A. Le Goff, M. Holzinger, *Electrochem. Commun.* **2014**, *38*, 19–23.

15 E. Katz, *Bioelectronic Medicine* **2015**, *2*, 1–12.

16 E. Katz, K. MacVittie, *Energy Environ. Sci.* **2013**, *6*, 2791–2803.

17 A. J. Bandodkar, J. Wang, *Electroanalysis* **2016**, *28*, 1188–1200.

18 A. J. Bandodkar, *J. Electrochem. Soc.* **2017**, *164*, H3007–H3014.

19 V. Coman, R. Ludwig, W. Harreither, D. Haltrich, L. Gorton, T. Ruzgas, S. A. Shleev, *Fuel Cells* **2010**, *10*, 9–16.

20 M. Southcott, K. MacVittie, J. Halámek, L. Halámková, W. D. Jemison, R. Lobel, E. Katz, *Phys. Chem. Chem. Phys.* **2013**, *15*, 6278–6283.

21 M. Cadet, S. Gounel, C. Stines-Chaumeil, X. Brilland, J. Rouhana, F. Louerat, N. Mano, *Biosens. Bioelectron.* **2016**, *83*, 60–67.

22 C. Pan, Y. Fang, H. Wu, M. Ahmad, Z. Luo, Q. Li, J. Xie, X. Yan, L. Wu, Z. L. Wang, J. Zhu, *Adv. Mater.* **2010**, *22*, 5388–5392.

23 D. Pankratov, L. Ohlsson, P. Gudmundsson, S. Halak, L. Ljunggren, Z. Blum, S. Shleev, *RSC Adv.* **2016**, *6*, 70215–70220.

24 M. Rasmussen, R. E. Ritzmann, I. Lee, A. J. Pollack, D. Scherson, *J. Am. Chem. Soc.* **2012**, *134*, 1458–1460.

25 L. Halámková, J. Halámek, V. Bocharova, A. Szczupak, L. Alfonta, E. Katz, *J. Am. Chem. Soc.* **2012**, *134*, 5040–5043.

26 A. Szczupak, J. Halámek, L. Halámková, V. Bocharova, L. Alfonta E. Katz, *Energy Environmen. Sci.* **2012**, *5*, 8891-8895.

27 K. MacVittie, J. Halámek, L. Halámková, M. Southcott, W. D. Jemison, R. Lobel, E. Katz, *Energy Environmen. Sci.* **2013**, *6*, 81–86.

28 J. A. Castorena-Gonzalez, C. Foote, K. MacVittie, J. Halámek, L. Halámková, L. A. Martinez-Lemus, E. Katz, *Electroanalysis* **2013**, *25*, 1579–1584.

29 P. Cinquin, C. Gondran, F. Giroud, S. Mazabrard, A. Pellissier, F. Boucher, J.-P. Alcaraz, K. Gorgy, F. Lenouvel, S. Mathe, P. Porcu, S. Cosnier, *PLOS ONE* **2010**, *5*, art. No. e10476.

30 S. El Ichi-Ribault, J.-P. Alcaraz, F. Boucher, B. Boutaud, R. Dalmolin, J. Boutonnat, P. Cinquin, A. Zebda, D. K. Martin, *Electrochim. Acta* **2018**, *269*, 360–366.

31 T. Miyake, K. Haneda, N. Nagai, Y. Yatagawa, H. Onami, S. Yoshino, T. Abe, M. Nishizawa, *Energy Environ. Sci.* **2011**, *4*, 5008–5012.

32 M. Falk, D. Pankratov, L. Lindh, T. Arnebrant, S. Shleev, *Fuel Cells* **2014**, *14*, 1050–1056.

33 A. J. Bandodkar, J.-M. You, N.-H. Kim, Y. Gu, R. Kumar, A. M. V. Mohan, J. Kurniawan, S. Imani, T. Nakagawa, B. Parish, M. Parthasarathy, P. P. Mercier, S. Xu, J. Wang, *Energy Environ. Sci.* **2017**, *10*, 1581–1589.

34 M. Falk, V. Andoralov, Z. Blum, J. Sotres, D. B. Suyatin, T. Ruzgas, T. Arnebrant, S. Shleev, *Biosens. Bioelectron.* **2012**, *37*, 38–45.

35 M. Falk, V. Andoralov, M. Maria Silow, M. D. Toscano, S. Shleev, *Anal. Chem.* **2013**, *85*, 6342−6348.

36 S. Cosnier, A. Le Goff, M. Holzinger, *Electrochem. Commun.* **2014**, *38*, 19–23.

37 F. Shen, D. Pankratov, G. Pankratova, M. D. Toscano, J. D. Zhang, J. Ulstrup, Q. J. Chi, L. Gorton, *Bioelectrochemistry* **2019**, *128*, 94–99.

38 X. X. Xiao, P. O. Conghaile, D. Leech, R. Ludwig, E. Magner, *Biosens. Bioelectron.* **2017**, *90*, 96–102.

39 A. G. Mark, E. Suraniti, J. Roche, H. Richter, A. Kuhn, N. Mano, P. Fischer, *Lab Chip* **2017**, *17*, 1761–1768.

40 K. Monsalve, I. Mazurenko, N. Lalaoui, A. Le Goff, M. Holzinger, P. Infossi, S. Nitsche, J. Y. Lojou, M. T. Giudici-Orticoni, S. Cosnier, E. Lojou, *Electrochem. Commun.* **2015**, *60*, 216–220.

41 A. Zebda, S. Cosnier, J. P. Alcaraz, M. Holzinger, A. Le Goff, C. Gondran, F. Boucher, F. Giroud, K. Gorgy, H. Lamraoui, P. Cinquin, *Sci. Rep.* **2013**, *3*, art. No. 1516.

42 M. Gamella, A. Koushanpour, E. Katz, *Bioelectrochemistry* **2018**, *119*, 33–42.

43 D. Pankratov, E. González-Arribas, Z. Blum, S. Shleev, *Electroanalysis* **2016**, *28*, 1250–1266.

44 Z. Xu, Y. Liu, I. Williams, Y. Li, F. Qian, L. Wang, Y. Lei, Baikun Li, *Appl. Energy* **2017**, *194*, 71–80.

45 M. Kizling, S. Draminska, K. Stolarczyk, P. Tammela, Z. Wang, L. Nyholm, R. Bilewicz, *Bioelectrochemistry* **2015**, *106*, 34–40.

46 K. Sode, T. Yamazaki, I. Lee, T. Hanashi, W. Tsugawa, *Biosens. Bioelectron.* **2016**, *76*, 20–28.

47 Y. Lee, S. Bang, I. Lee, Y. Kim, G. Kim, M. H. Ghaed, P. Pannuto, P. Dutta, D. Sylvester, D. Blaauw, *IEEE J. Solid-State Circuits* **2013**, *48*, 229–243.

48 B. Warneke, M. Last, B. Liebowitz, K. S. J. Pister, *Computer* **2001**, *34*, 44–51.

49 S. Oh, Y. Lee, J. Wang, Z. Foo, Y. Kim, W. Jung, Z. Li, D. Blaauw, D. Sylvester, *IEEE J. Solid-State Circuits* **2015**, *50*, 1581–1591.

50 W. Jung, S. Oh, S. Bang, Y. Lee, Z. Foo, G. Kim, Y. Zhang, D. Sylvester, D. Blaauw, *IEEE J. Solid-State Circuits* **2014**, *49*, 2800–2811.

51 I. Lee, Y. Lee, D. Sylvester, D. Blaauw, *IEEE J. Solid-State Circuits* **2016**, *51*, 2743–2756.

52 Gray garden slug *Deroceras reticulatum* fact sheet: http://idtools.org/id/mollusc/factsheet.php?name=Deroceras%20reticulatum

53 G. Fusco, G. Göbel, R. Zanoni, E. Kornejew, G. Favero, F. Mazzei, F. Lisdat, *Electrochim. Acta* **2017**, *248*, 64–74.

54 G. Fusco, G. Göbel, R. Zanoni, M. P. Bracciale, G. Favero, F. Mazzei, F. Lisdat, *Biosens. Bioelectron.* **2018**, *112*, 8–17.

55 W. Jung, J. Gu, P. D. Myers, M. Shim, S. Jeong, K. Yang, M. Choi, Z. Foo, S. Bang, S. Oh, D. Sylvester, D. Blaauw, *IEEE International Solid-State Circuits Conference (ISSCC)*, San Francisco, CA, **2016**, pp. 154–155.

56 K. Yang, Q. Dong, W. Jung, Y. Zhang, M. Choi, D. Blaauw, D. Sylvester, *IEEE International Solid-State Circuits Conference (ISSCC)*, San Francisco, CA, **2017**, pp. 160–161.

57 T. Jang, M. Choi, S. Jeong, S. Bang, D. Sylvester, D. Blaauw, *IEEE International Solid-State Circuits Conference (ISSCC)*, San Francisco, CA, **2016**, pp. 102–103.

58 Y. Shi, M. Choi, Z. Li, Z. Luo, G. Kim, Z. Foo, H.-S. Kim, D. Wentzloff, D. Blaauw, *IEEE J. Solid-State Circuits* ***2016***, *51*, 2570–2583.

59 G. Göbel, I. W. Schubart, V. Scherbahn, F. Lisdat, *Electrochem. Commun.* **2011**, *13*, 1240–1243.

60 V. Wernert, C. Lebouin, V. Benoit, R. Gadiou, A. de Poulpiquet, E. Lojou, R. Denoyel, *Electrochim. Acta* **2018**, *283*, 88–96.

61 U. Salaj-Kosla, S. Pöller, Y. Beyl, M. D. Scanlon, S. Beloshapkin, S. Shleev, W. Schuhmann, E. Magner, *Electrochem. Commun.* **2012**, *16*, 92–95.

62 V. Scherbahn, M. T. Putze, B. Dietzel, T. Heinlein, J. J. Schneider, F. Lisdat, *Biosens. Bioelectron.* **2014**, *61*, 631–638.

63 C. Walgama, A. Pathiranage, M. Akinwale, R. Montealegre, J. Niroula, E. Echeverria, D. N. McIlroy, T. A. Harriman, D. A. Lucca, S. Krishnan, *ACS Appl. Bio. Mater.* **2019**, *2*, 2229–2236.

64 A. J. Gross, M. Holzinger, S. Cosnier, *Energy Environ. Sci.* **2018**, *11*, 1670–1687.

65 A. J. Gross, M. Holzinger, S. Cosnier, in: S. Cosnier (Ed.), *Bioelectrochemistry. Design and Application of Biomaterials*. Ch. 1, pp. 1-22, De Gruyter, **2019**.

66 Y. Holade, K. MacVittie, T. Conlon, N. Guz, K. Servat, T. W. Napporn, K. B. Kokoh, E. Katz, *Electroanalysis* **2014**, *26*, 2445–2457.

67 A. Nowakowska, M. Caputa, J. Rogalska, *J. Physiol. Pharmacol.* **2006**, *57*, 93–105.

68 B. Reuillard, C. Abreu, N. Lalaoui, A. Le Goff, M. Holzinger, O. Ondel, F. Buret, S. Cosnier, *Bioelectrochemistry* **2015**, *106*, 73–76.

69 B. I. Rapoport, J. T. Kedzierski, R. Sarpeshkar, *PLOS ONE* **2012**, *7*, art. No. e38436.

70 Y. Holade, K. MacVittie, T. Conlon, N. Guz, K. Servat, T. W. Napporn, K. B. Kokoh, E. Katz, *Electroanalysis* **2015**, *27*, 276–280.

71 S. Kerzenmacher, J. Ducrée, R. Zengerle, F. von Stetten, *J. Power Sources* **2008**, *182*, 1–17.

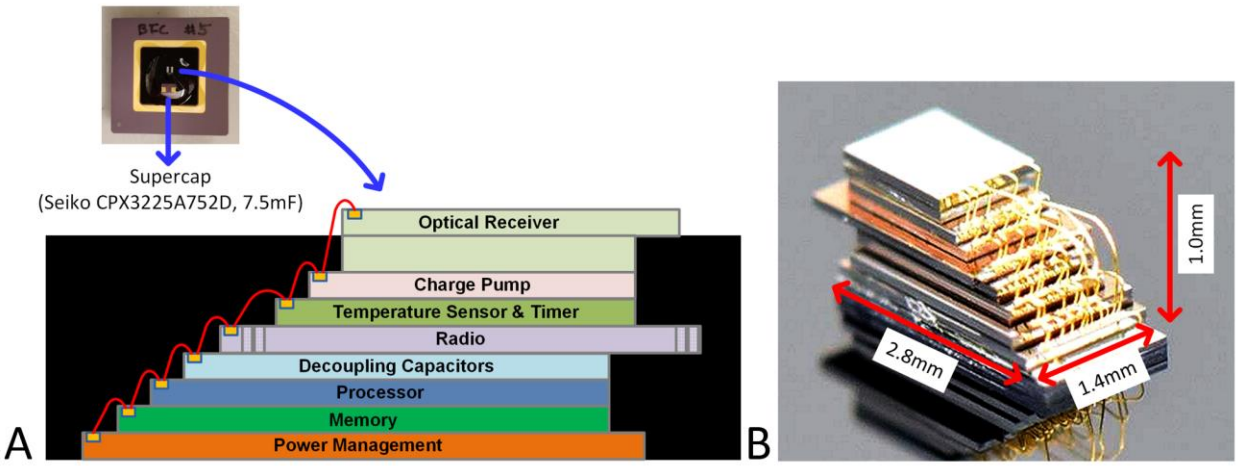

Figure 1. (A) The microelectronic temperature-sensing device schematic composition. (B) The stack of the chips (without encapsulation).

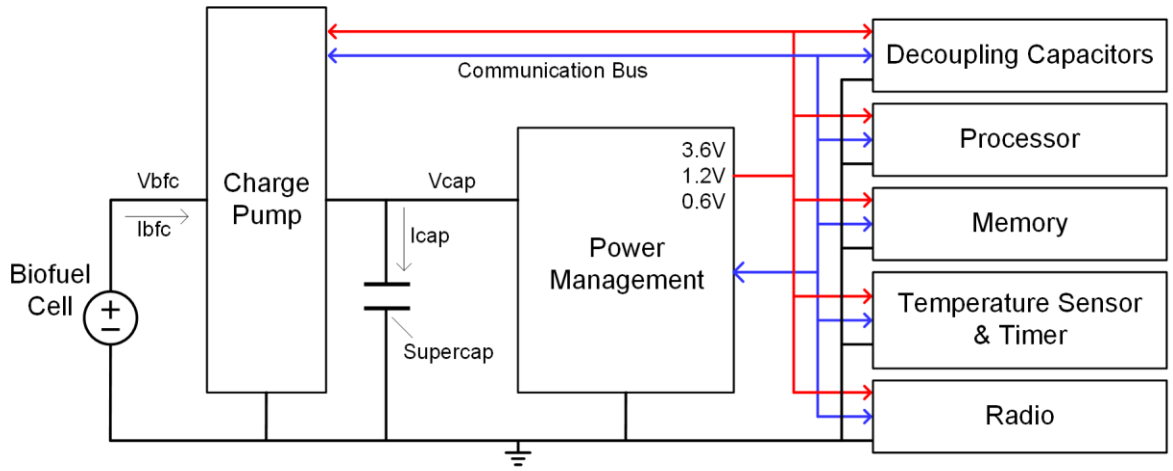

Figure 2. The electronic block scheme of the microelectronic temperature-sensing device powered by the biofuel cell. A charge pump chip converts the low voltage of the biofuel cell to voltage acceptable for operating electronic circuits. The power management chip (also containing up/down charge pumps internally) generates three stabilized voltages for the different load circuits.

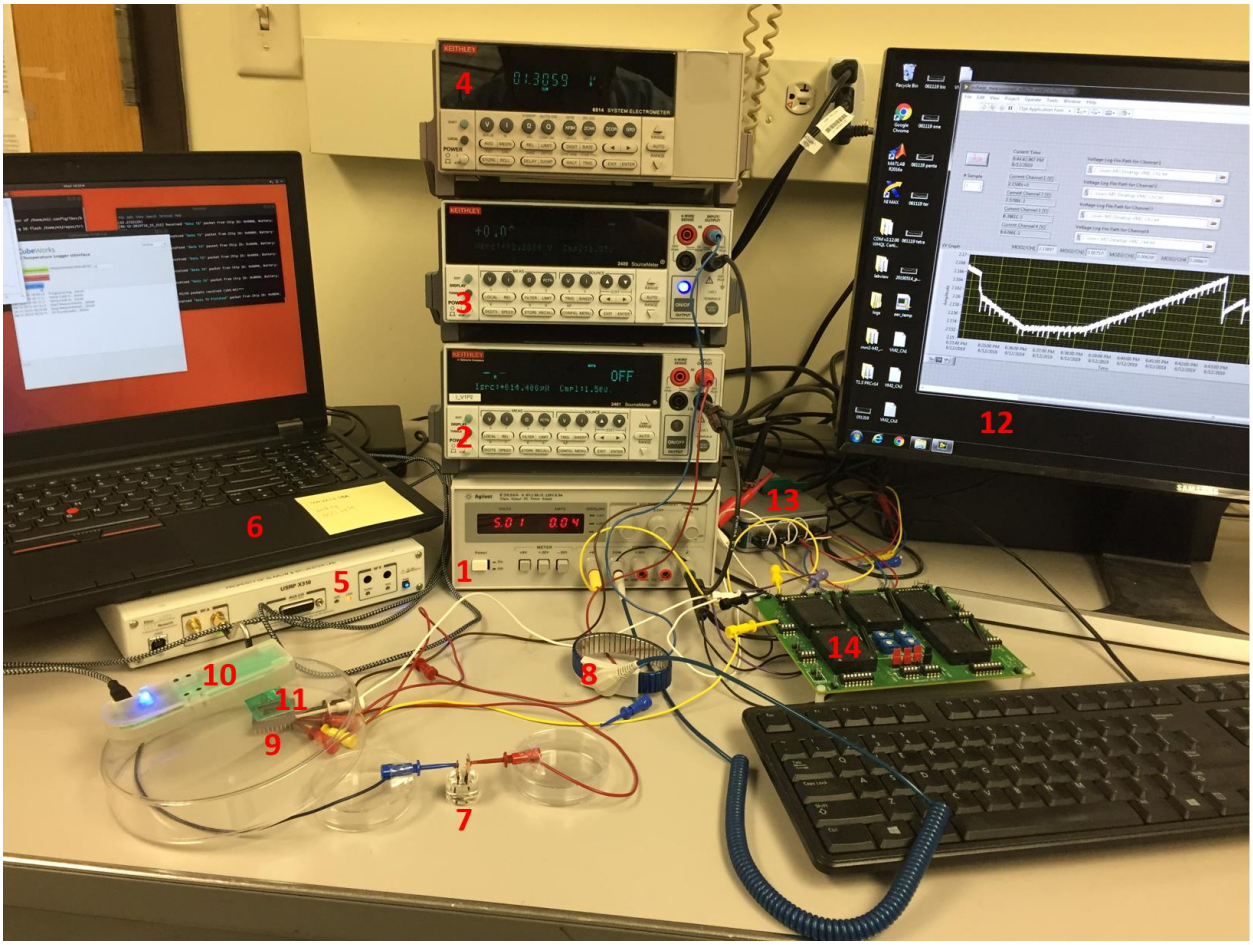

Figure 3. The experimental setup for studying the microelectronic device operation and characterizing its different components. See the setup description in Section 2.5. The numbered parts of the experimental setup are as follows:

(1) power supply (Agilent E3630A);

(2) sourcemeter (Keithely 2401 Sourcemeter) used in preliminary experiments (data not reported) to mimic the real biofuel cell;

(3) sourcemeter (Keithely 2400 Sourcemeter) needed to charge the supercapacitor (Seiko CPX3225A752D, 7.5 mF);

(4) electrometer (Keithely 6514 System Electrometer) to monitor voltages of the M3 sensor;

(5) universal software radio peripheral (USRP) (Ettus, USRP X310);

(6) laptop (Lenovo P51) equipped with custom programing software;

(7) biofuel cell operating with a model aqueous solution, replaced with a live slug in the final system test;

(8) anti-static wrist (ESD) strap used by an operator;

(9) microelectronic sensor device;

(10) custom light programing module;

(11) custom printed circuit board (PCB) antenna for base station;

(12) desktop computer using a LABVIEW program;

(13) analog-to-digital converter module (National Instruments, NI-9229 & NI cDAQ-9171);

(14) analog buffer PCB (Texas Instruments, OPA4354AIDR)

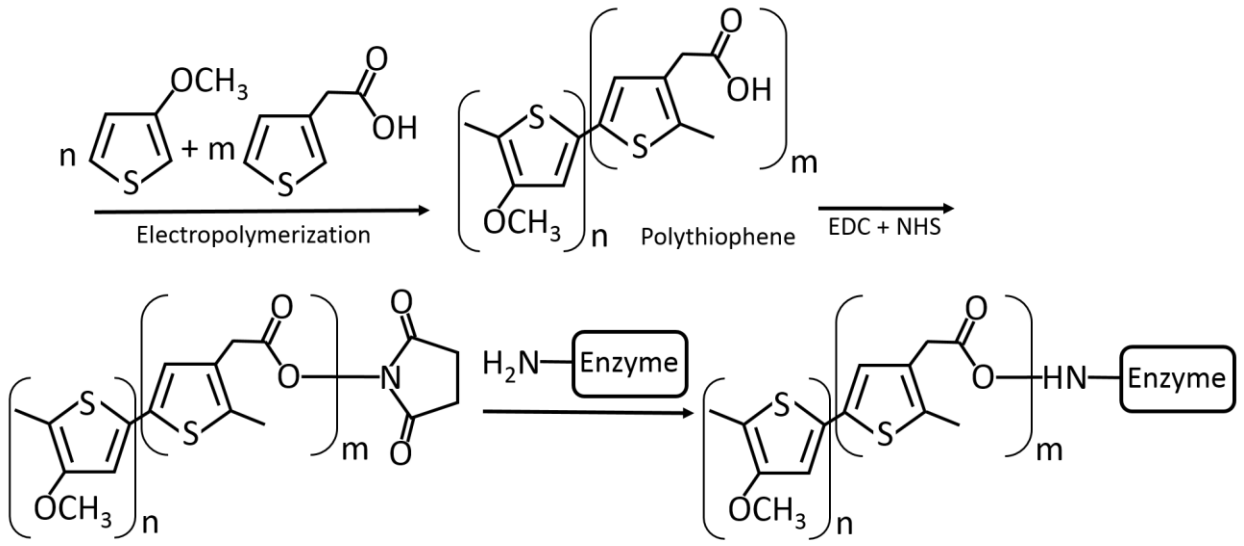

Figure 4. The scheme showing preparation of the electropolymerized polythiophene sub-layer, further modified with covalently bound enzymes. Note the ratio of the original thiophene-monomers n : m = 2 : 1.

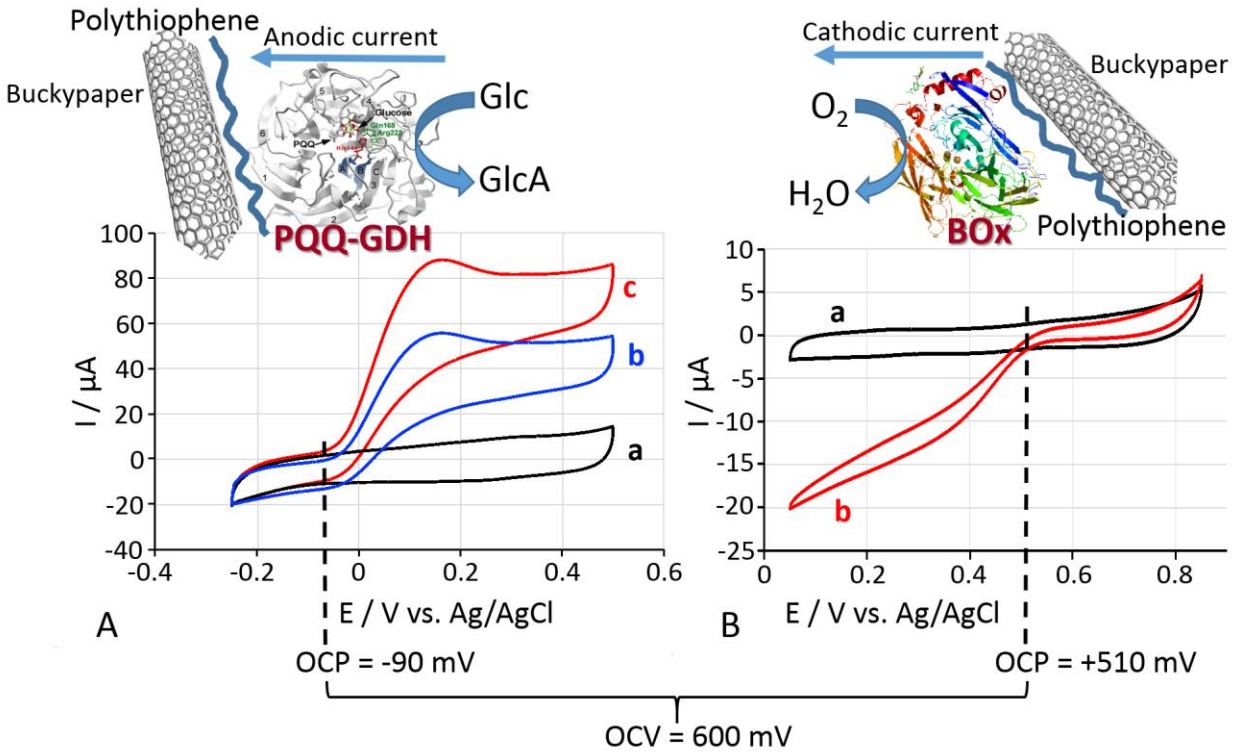

Figure 5. (A) Cyclic voltammograms obtained with the PQQ-GDH-modified electrode measured in the absence (a) and presence of glucose, 5 mM (b) and 20 mM (c). (B) Cyclic voltammograms obtained with the BOx-modified electrode measured under anaerobic conditions (a) and in the presence of O_2 (in equilibrium with air) (b). Background electrolyte was 50 mM phosphate buffer, pH 7.4, containing 100 mM Na_2SO_4. Potential scan rate was 1 $mV \cdot s^{-1}$. Abbreviations used: PQQ-GDH – PQQ-dependent glucose dehydrogenase, BOx – bilirubin oxidase, Glc – glucose, GlcA – gluconic acid (product of Glc biocatalytic oxidation), OCP – open circuit potential (measured vs. the reference electrode), OCV – open circuit voltage (measured between two biocatalytic electrodes).

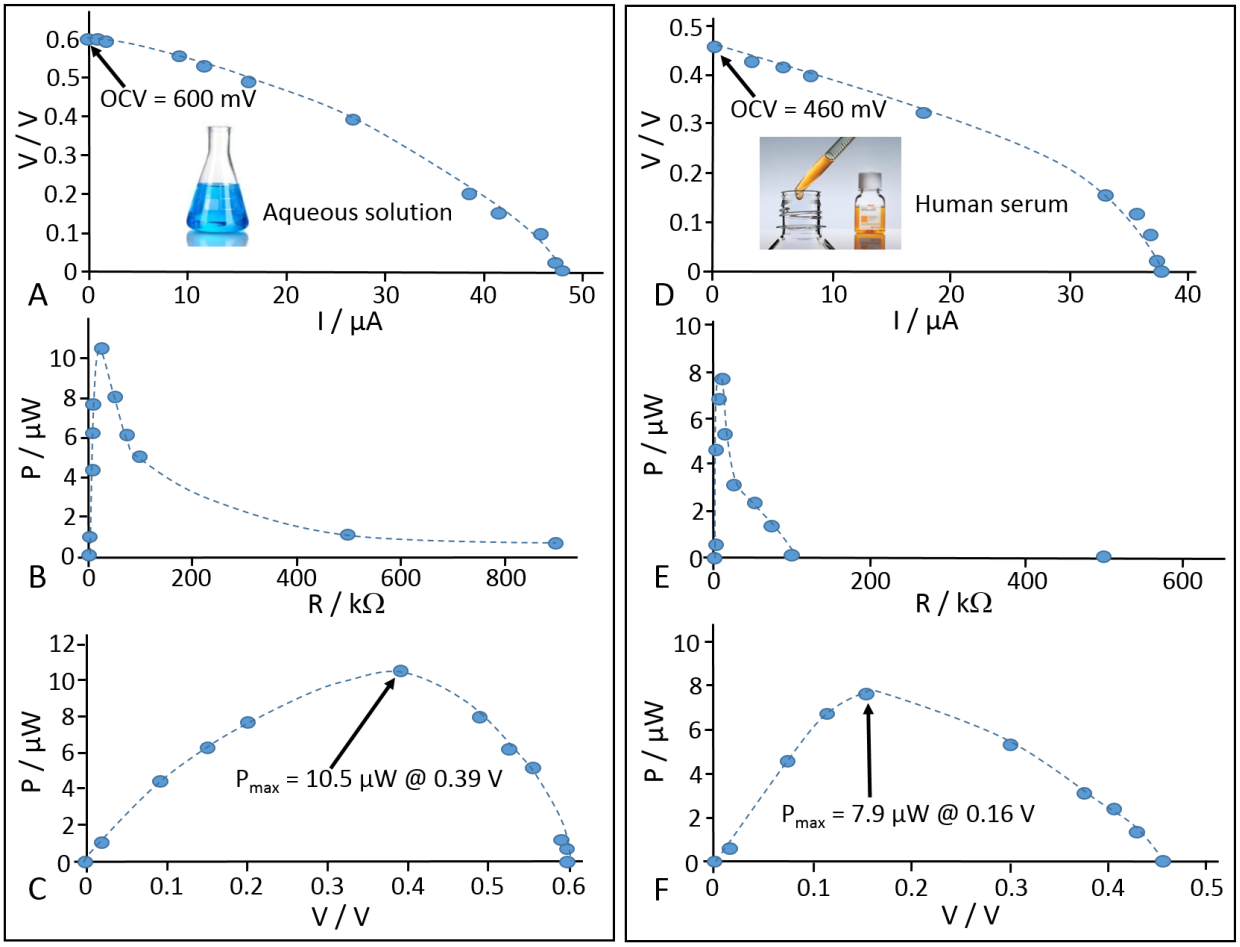

Figure 6. Biofuel cell polarization curves and power release measured: (A-C) with 50 mM phosphate buffer, pH 7.3, containing 100 mM Na_2SO_4 and 20 mM glucose; (D-F) with human serum containing ca. 6 mM glucose. Oxygen was always present under equilibrium with air. The circles in the plots reflect the experimental distribution of the measured parameters.

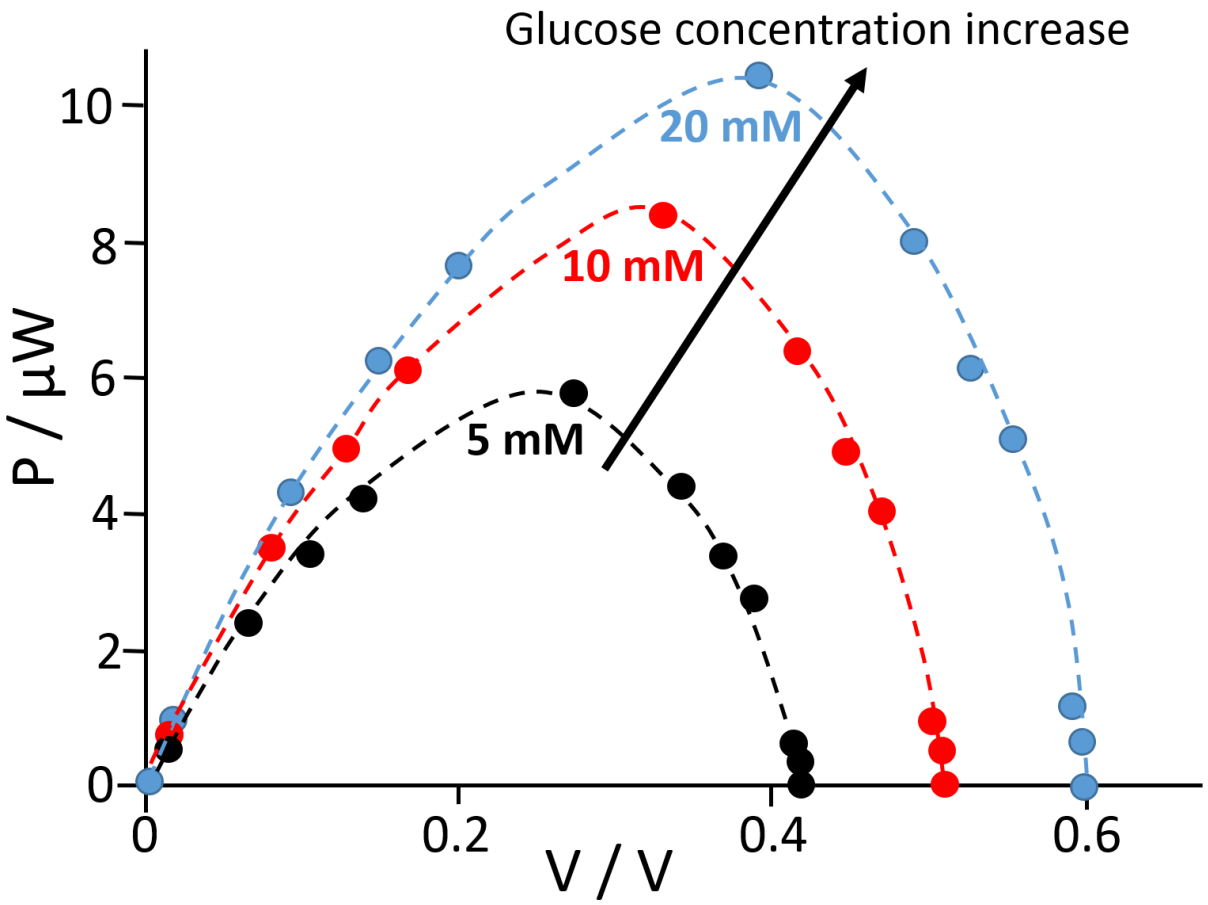

Figure 7. Power release function measured with the biofuel cell filled with 50 mM phosphate buffer, pH 7.3, containing 100 mM Na_2SO_4 and different concentrations of glucose: 5 mM, 10 mM and 20 mM. Oxygen was always present under equilibrium with air. The circles in the plots reflect the experimental distribution of the measured parameters.

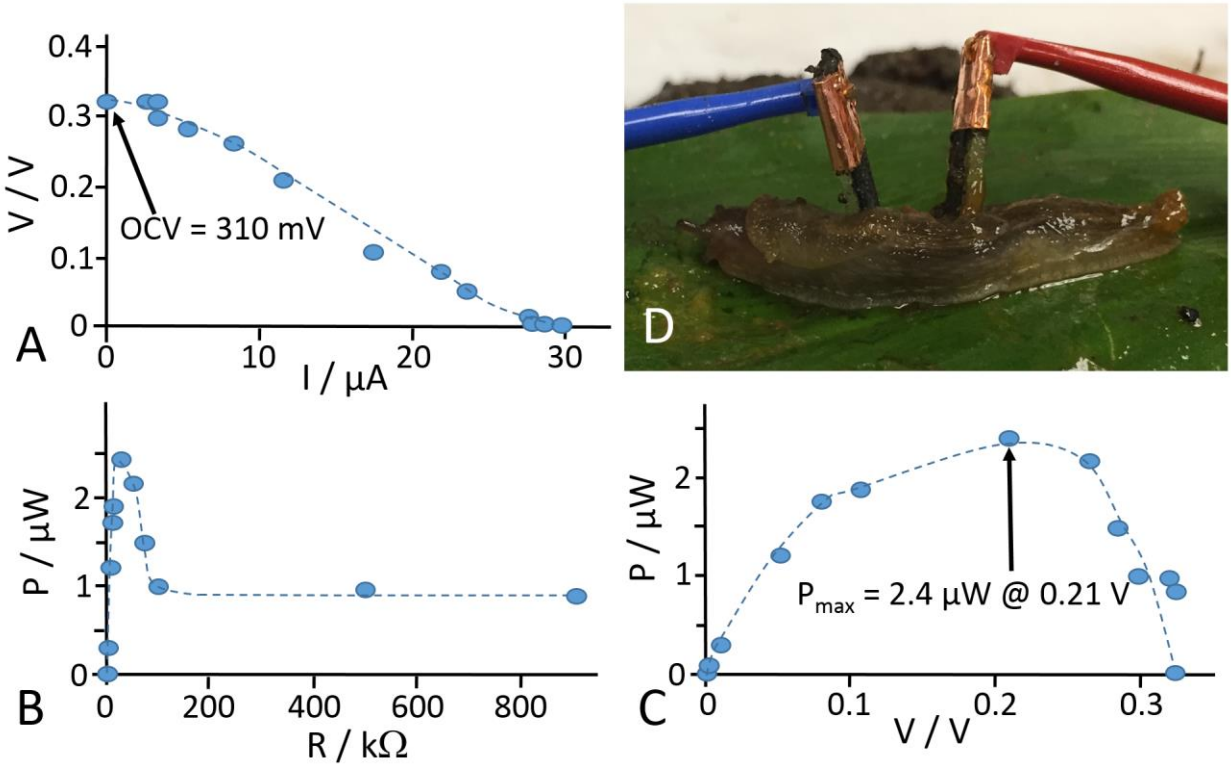

Figure 8. Biofuel cell polarization curve (A) and power release functions (B-C) measured with the biocatalytic electrodes implanted in a living slug (D). The circles in the plots reflect the experimental distribution of the measured parameters.

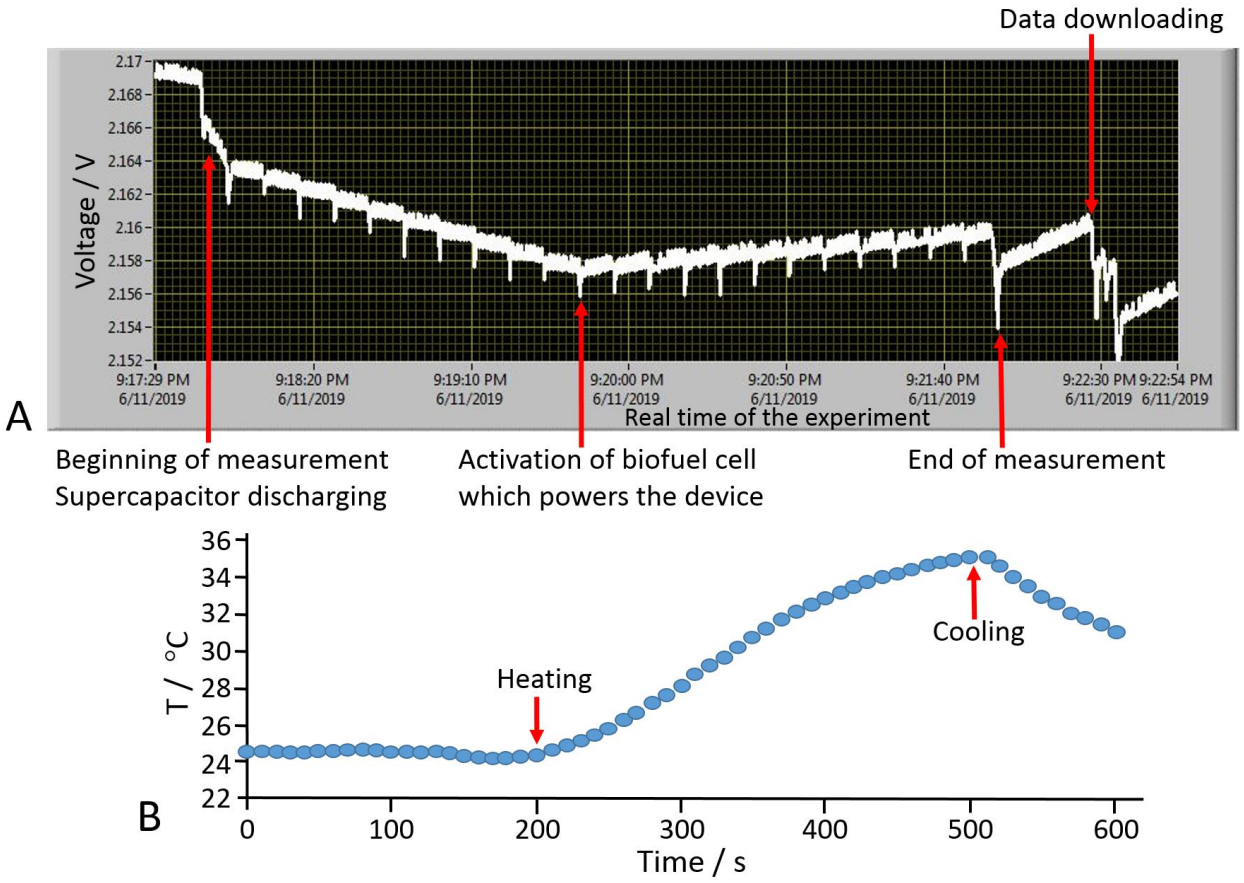

Figure 9. (A) Measured voltage (Vcap in Figure 2) of the supercapacitor in the miniature energy-autonomous temperature sensor powered only by the biofuel cell. (B) Temperature measurements recorded by the sensor powered by the biofuel cell and read out wirelessly ("data recording") from the sensor. Icap, Vbfc and Ibfc are –525 nA, 0.31 V, 0 A before 'Activation of biofuel cell' and 196 nA, 0.21 V, 11.4 µA after 'Activation of biofuel cell' (see the calculation of these electrical parameters in the Supporting Information).

Graphical Abstract

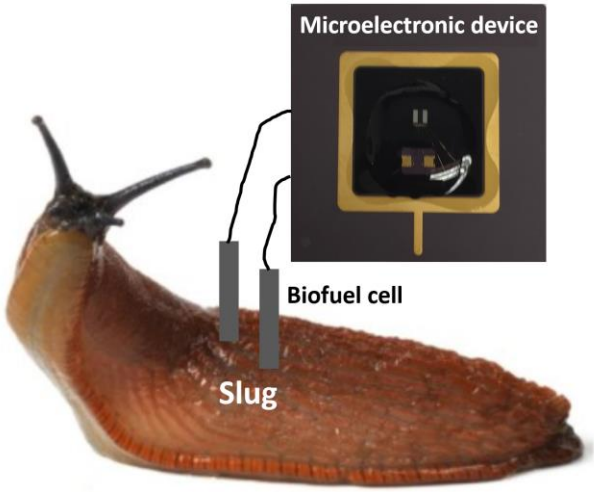

Table of contents entry:

A microelectronic sensor device was powered by an enzyme biofuel cell implanted in a slug to operate autonomously.